J Mater Sci: Mater Med (2010) 21:259–266
DOI 10.1007/s10856-009-3832-z

Structure, morphology and fibroblasts adhesion of surface-porous titanium via anodic oxidation

Li Xie · Guangfu Yin · Danhong Yan · Xiaoming Liao · Zhongbing Huang · Yadong Yao · Yunqing Kang · Yao Liu

Received: 23 April 2009 / Accepted: 20 July 2009 / Published online: 30 July 2009

Abstract Surface-porous titanium samples were prepared by anodic oxidation in H_2SO_4, H_3PO_4 and CH_3COOH electrolytes under various electrochemical conditions. X-ray diffraction (XRD), scanning electron microscopy (SEM) and energy dispersive X-ray spectroscopy (EDX) were employed to characterize the structure, morphology and chemical composition of the surface layer, respectively. Closer analysis on the effect of the electrochemical conditions on pore configuration was involved. It can be indicated that porous titania was formed on the surface layer, and the pore configuration was influenced by electrolyte composition and crystal structure of the titania. The fibroblast cells experiment showed that anodic oxidation of titanium surface could promote fibroblast adhesion on Ti substrate. The results suggested that anodic oxidation of Ti in CH_3COOH was suitable to obtain surface-porous titanium oxides layers, which might be beneficial for better soft tissue ingrowths.

1 Introduction

Titanium and its alloys have been widely used as artificial implant materials in dental, maxillofacial, bone replacement and orthopaedic surgery due to their excellent mechanical, chemical properties and biocompatibility [1–3]. However, as a bioinert metallic material, titanium implants can not form direct bonds with living bone [4]. Therefore, various methods such as plasma-sprayed HA-coating [5], NaOH and heat treatment [6–8], anodic oxidation [9–12] have been developed to improve the bioactivity of titanium metals.

As known to all, in certain orthopaedic reconstructive procedures, it would be beneficial for implants to possess porous structure that enables attachment to both bone and soft tissues [13]. This includes tendon and ligament reattachment in both upper and lower extremities [14] and tissue attachment for custom devices used for salvaging joint reconstructions [15] or tumor replacement prostheses [16]. In some occasions, most of outer surfaces of the implants are in contact with soft tissues. In order to allow soft tissue ingrowths, many different porous coated and bulk porous titanium implants have been developed by various methods [17–22]. But problems such as drastic reduction in fatigue strength [23] and difficulty to fabric fitting complex-surface implants have not been resolved [24].

Recently, anodic oxidation (AO) has become an attractive method to obtain rough, porous titania layer on titanium surface, which is proper to improve the bioactivity of the substrate [9–12]. Moreover, it can be readily applied to implants with complex surface patterns [25] and the structural and chemical properties of anodic layer can be controlled by altering electrochemical parameters [11]. In previous reports, it was shown that anodic oxidation could be carried out in various electrolytes and the maximum pore size is several microns [12, 26–30], which is rather small for soft tissue ingrowths [31]. Recently, most of the studies focus on the apatite-forming ability assessment of AO Ti in SBF [9–12]. However, further analysis of surface morphology and crystal structure, especially pore configuration has been few reported, which might be essential to develop better surface-porous implants.

In this paper, the morphology and crystal structure of the AO surface-porous titanium, especially the influence of the

L. Xie · G. Yin · D. Yan · X. Liao (✉) · Z. Huang · Y. Yao · Y. Kang · Y. Liu
College of Materials Science and Engineering, Sichuan University, Chengdu 610064, People's Republic of China
e-mail: sherman_xm@163.com

electrochemical parameters on the pore configuration, were investigated after treated in H_2SO_4, H_3PO_4 and CH_3COOH electrolytes. A heterogenous larger porous-structure amorphous titanium oxides layer on Ti substrate was prepared in CH_3COOH electrolyte. In addition, fibroblasts adhesion properties in short-term culture on anodized titanium surfaces were discussed.

2 Materials and methods

2.1 Anodic oxidation

Commercially pure titanium (TA2) samples, with the size of 10 × 10 × 1 mm, were carefully polished with No. 400, 600, and 700 metallographic abrasive paper, then the samples were ultrasonically cleaned with pure acetone, ethanol, and distilled water for 5 min, respectively. Anodic oxidation was carried out at room temperature with a direct current power supply system (QUERLI DC Power Supply WYJ-500 V 1 A, China). The conditions of anodic oxidation were given in Table 1. Two rectangular titanium plates, 300 × 3 × 1 mm and 300 × 10 × 1 mm in size, were used as anode and cathode, respectively. A rectangular slot with a size 1.5 × 4.0 mm was made in the lower end of the anode to fix the titanium sample. The electrolyte was contained in a glass vessel of capacity 500 cm^3. Only the anode titanium samples fixed in the slot immerged in the electrolyte and the opposite cathode area immerged in the solution was about 30 × 10 mm. During the anodic oxidation process, a magnetic stirrer at a given rotation speed was employed to achieve a homogeneous electrolyte and to accelerate escape of gas produced in the electrochemical reaction from the surface of the titanium substrates. After the anodic oxidation, the samples were rinsed with distilled water and dried with an air drier. The surface morphologies of the AO samples were observed using a scanning electron microscopy (SEM; Hitachi, S-4800). The crystallographic characteristic of the surface-porous layer was investigated by X-ray diffraction (XRD; Philips, X'Pert MPD 3 kW). The surface chemical compositions of samples anodized at 180 V for 1 min in 1 M H_2SO_4 (named S180), 2 M H_3PO_4 (named P180) and 2 M CH_3COOH (named C180) were checked by the attached energy dispersive X-ray spectroscopy (EDX) of Hitachi SEM S-4800.

2.2 Fibroblast cells culture

The substrates, modified by anodic oxidation (the untreated titanium sample was used as control), were ultrasonically cleaned with doubly distilled water, washed with phosphate buffered saline (PBS) solution and then sterilized in autoclave at 121°C for 20 min, prior to being placed into the wells of a 24-well culture plate. L929 fibroblasts (provided by College of Life Science, Sichuan University) were seeded into the wells at a density of 1 × 10^4 cells/well and incubated in 1 ml of Dulbecco's modified Eagle's medium (DMEM) supplemented with 10% fetal bovine serum, 1 mM L-glutamine, and 100 U/ml penicillin (diluted from the 20,000 U/ml stock solution) at 37°C under a humidified 5% CO_2 atmosphere. The surfaces after 24 h of incubation were washed with PBS solution to remove the loosely adsorbed cells. Fixation of cells with 4% glutaraldehyde in PBS for 4 h at 4°C, followed by dehydration with 25, 50, 70, and 95% (v/v) ethanol solutions for 15 min, respectively, with final dehydration in absolute ethanol twice. The surfaces with immobilized cells were then dried in supercritical carbon dioxide and sputter-coated with a thin film of gold prior to SEM (JEOL, JSM-5900LV) imaging.

3 Results and discussion

3.1 Surface morphology, crystal structure and chemical composition of AO titanium

Figure 1 illustrates the surface SEM micrographs of untreated titanium and anodically oxidized titanium in 1 M H_2SO_4 for 1 min at different voltages. The surface of

Table 1 The concentration of electrolytes and the anodizing conditions

Electrolyte	Concentration (M)	Final voltage (V)	Current density (mA/cm^2)	Anodizing time (min)*
H_2SO_4	1	90	25	5; 1
	1	155	100	11; 1
	1	180	140	18; 1
H_3PO_4	2	100	20	1.5; 1
	2	150	25	2; 1
	2	180	30	2.5; 1
CH_3COOH	2	100	15	6; 1
	2	150	35	15; 1
	2	180	50	17; 1

* Anodizing time includes two parts, the former is time to reach the current density, the latter is duration time at final voltage

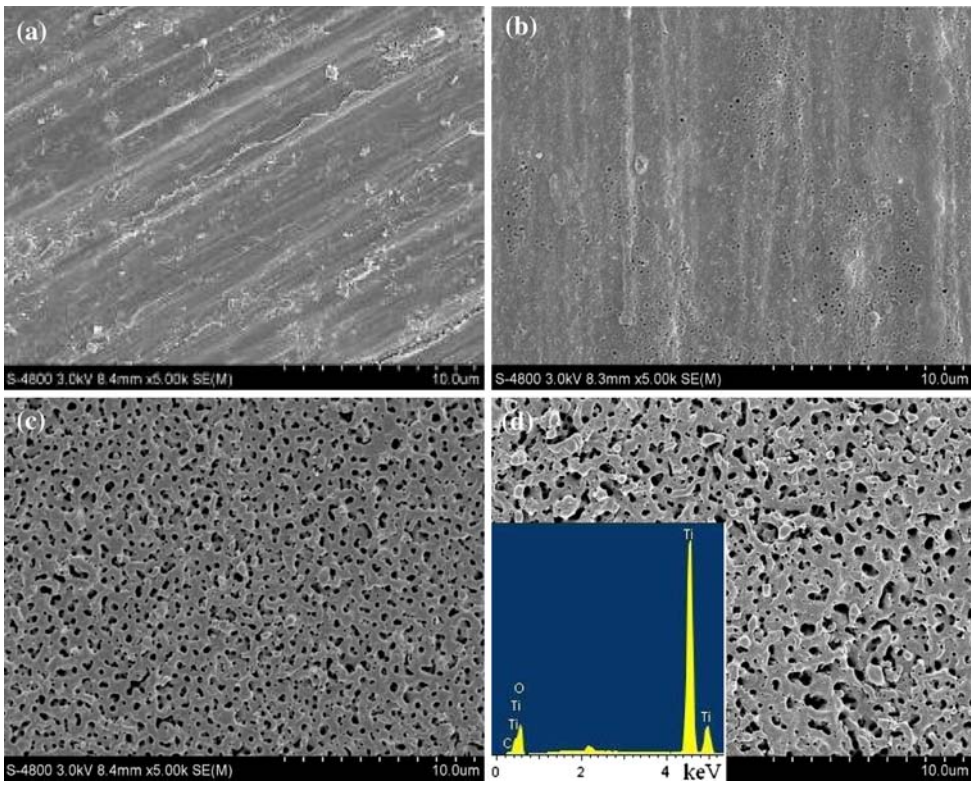

Fig. 1 SEM micrographs of titanium untreated (**a**) and anodized in 1 M H_2SO_4 for 1 min at **b** 90 V, **c** 155 V, **d** 180 V, the inset is an EDX spectrum of the surface layer

untreated titanium was consisted of scratches formed during mechanical grounding, as shown in Fig. 1a. At applied voltage 90 V (Fig. 1b), scratches were not visible and the surface layer was uniform, comprising a few areas with small pores of size less than 200 nm and the numerous areas without pores. In contrast, when applied voltages increased to 155 V, an obvious change in surface morphology was observed. A lot of pores, with size ranging from several nanometers to 1 μm, were well separated and evenly distributed on the surface. Further raising the voltage to 180 V, the porous structure did not change obviously.

Figure 2 is the XRD patterns of untreated titanium and anodically oxidized titanium in 1 M H_2SO_4 for 1 min at different voltages. From Fig. 2a, only the peaks of titanium could be observed for the untreated Ti sample. The peaks of anatase phase appeared for the titanium samples oxidized at 90 V (Fig. 2b). A further increase in voltage resulted in an increase in the peak intensity of the anatase and rutile phase. From Fig. 2c, d, it can also be seen that the intensity of the peaks from the anatase phase and the titanium substrate decreased when applied voltage increasing from 155 to 180 V, while the intensity of the peaks from the rutile phase increased. The predominance of the X-ray peak at $2\theta = 27.7^{\circ}$ in XRD pattern at 180 V was assigned to rutile phase (shown in Fig. 2d). EDX analysis showed that S element was not detected on the surface of the sample anodized in 1 M H_2SO_4 at 180 V (S180), suggesting that S was not incorporated into the surfaces of AO Ti prepared in H_2SO_4.

Figure 3 illustrates the surface SEM micrographs of treated titanium samples via anodic oxidation in 2 M H_3PO_4 for 1 min at different voltages. The surface layers produced at any voltage were uniform and flattened, compared with SEM micrographs of titanium substrates anodized in H_2SO_4 electrolyte (Fig. 1). It can be observed that numerous round-like pores, with size ranging from several nanometers to 1 μm, were evenly distributed on the surface layer at all samples. The size of the pores increased with increasing voltage from 100 to 180 V, which is up to about 200 nm, 0.5 μm and 1 μm, respectively.

Figure 4 shows XRD patterns of titanium substrates via anodic oxidation in 2 M H_3PO_4 and 2 M CH_3COOH for 1 min at different voltages, respectively. All the patterns can be assigned as those arising from the diffraction of titanium. No peaks from anatase or rutile phase appeared. From the EDX spectra (shown in the inset of Figs. 3c, 4d), Ti, O, P, C were detected on the surface of the sample anodized in 2 M H_3PO_4 at 180 V (P180) at atomic percentages 31.94, 63.85, 2.21 and 2.0, respectively (Table 2). Ti, O and C were detected on the surface of the sample anodized in 2 M CH_3COOH at 180 V (C180) at atomic percentages 36.40, 58.11 and 5.48, respectively (Table 2). The Ti/O ratios of P180 and C180 were 0.50 and 0.63, respectively. Moreover, No crystalline TiO_2 peaks were observed in the XRD diffraction patterns of the

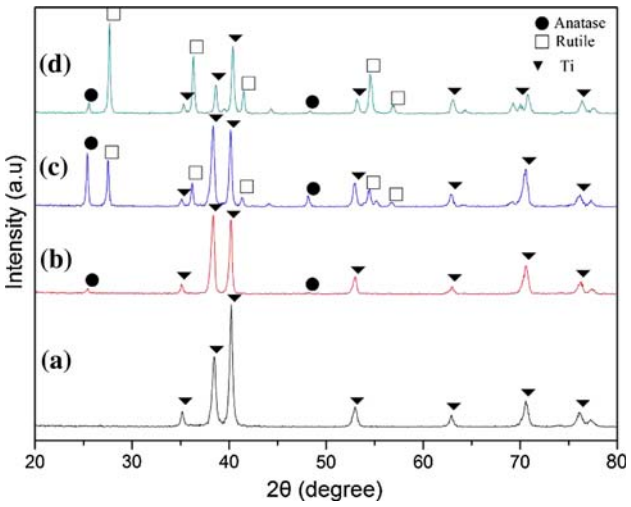

Fig. 2 XRD patterns of titanium untreated (a) and anodized at b 90 V, c 155 V, d 180 V in 1 M H_2SO_4 for 1 min

investigated samples. Thus, it can be concluded that amorphous TiO_2 has formed on the surface layers of P180 and C180.

Figure 5 is the SEM micrographs of titanium samples anodically oxidized in 2 M CH_3COOH. A distinct change in surface morphology was observed in comparison with the samples anodized in H_2SO_4 (Fig. 1) and H_3PO_4 (Fig. 3) electrolytes. It can be seen that the surface was relatively heterogenous in structure, consisting of some areas with severely etched turbinate-like craters with diameter about 10 μm and grooves with length about 200 μm (Fig. 5a, marked by white arrow), other areas with relatively smaller pores which ranged between 1 and 3 μm (Fig. 5b–d). Figure 5b, c, d illustrate that the quantity and size of the smaller pores on treated Ti samples increased with increasing voltage from 100 to 180 V. The larger pore sizes are about 2, 2.5 and 3 μm, respectively. The quantity of the pores was less than those via anodic oxidation in H_2SO_4 (Fig. 1). Moreover, from the inset in Fig. 5a, b (marked by white arrow), it can be observed that both the small pores and craters showed nano-size porous-structure rough edges. The depth of the crater is more than 10 μm according to Fig. 5a, suggesting that the thickness of the titanium oxides layer is not less than 10 μm.

The formation of the anodic titanium oxides layer appears as a competition between the solid titanium oxides layer growth and the dissolution of that layer at its interface with the electrolyte. The initial structure of anodic layer is amorphous, and it will change to crystalline phase when the anodic voltage is above breakdown value [32, 33]. Furthermore, it is known that anatase phase, stable at low temperature, is converted into rutile structure when heated above 915°C [34].

When anodized in H_2SO_4 electrolyte, spark discharges were observed on the surfaces of the substrates when applied voltage increased to above 100 V, and more intensive sparks were observed with increasing anodizing voltage. The instantaneous temperature and pressure in those small discharge zones (channels) can reach 10^3–10^4 K and 10^2–10^3 MPa, respectively [33]. Therefore, the

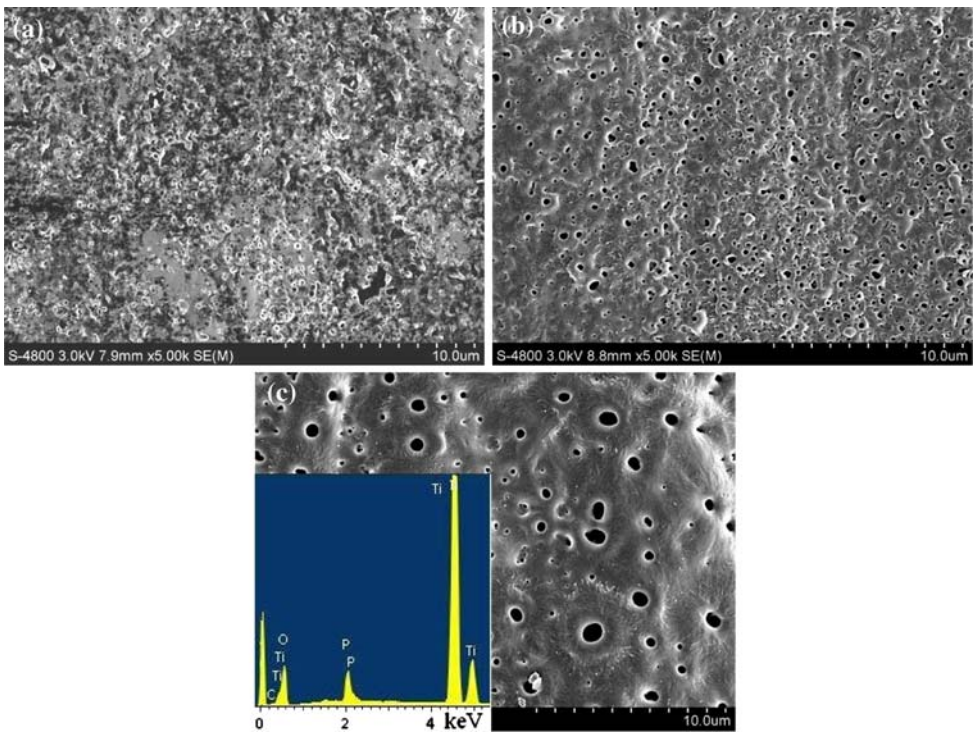

Fig. 3 SEM micrographs of titanium anodized in 2 M H_3PO_4 for 1 min at **a** 100 V, **b** 150 V, **c** 180 V, the inset is an EDX spectrum of the surface layer

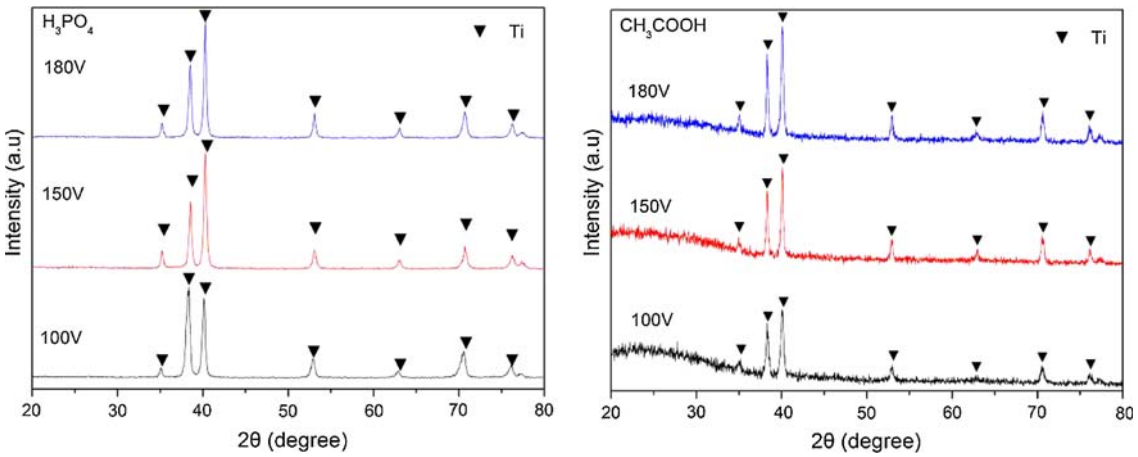

Fig. 4 XRD patterns of titanium anodized at 100, 150 and 180 V in 2 M H_3PO_4 and 2 M CH_3COOH for 1 min

Table 2 Chemical composition percents from EDX analysis of the anodized surfaces in different samples

Samples	Element					
	Ti	O	C	S	P	Ti/O
S180	29.47	66.85	3.67	–	–	0.44
P180	31.94	63.85	2.00	–	2.21	0.50
C180	36.40	58.11	5.48	–	–	0.63
unit: atomic %						

initially formed amorphous titania transformed into anatase, and anatase converted subsequently to rutile structure when applied voltage increased, which was consistent with XRD results. When anodized in H_3PO_4 electrolyte, spark discharge could be seen when applied voltage was above 140 V, but was very weak. When anodized in CH_3COOH electrolyte, spark discharge couldn't be observed on the surface of the titanium samples on the given conditions, consistent with previous similar findings of Sul et al. [29]. Therefore, the titanium oxides layers formed in H_3PO_4 and CH_3COOH electrolytes were still amorphous (Fig. 4).

The titanium oxides layer dissolution includes field assisted and chemical dissolution, especially the former. From the previous reports [25], it is known that there are three phases of titanium dioxide, anatase, rutile, and brookite. Among them, rutile is the most dense and stable phase and has been shown to increase the dissolution

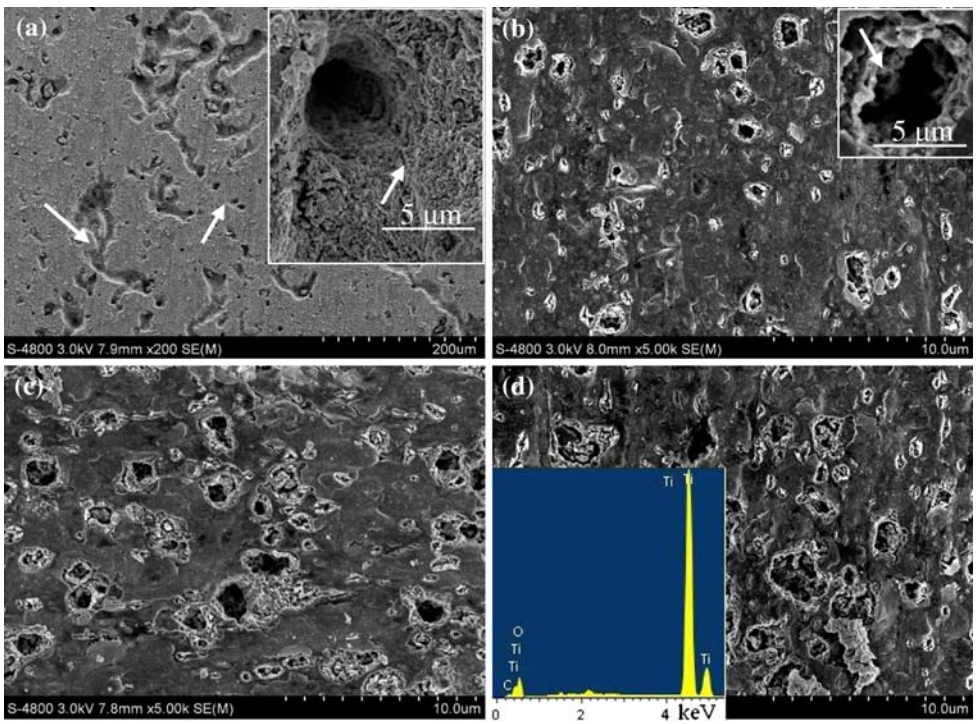

Fig. 5 SEM micrographs of titanium anodized in 2 M CH_3COOH for 1 min at **a** 180 V, **b** 100 V, **c** 150 V, **d** 180 V. Insets are high-magnification micrographs and the EDX spectrum of the surface layer, respectively

resistance, so it can be concluded that the dissolution resistance of titania phases may satisfy the following inequation.

$$R_{ru} > R_{an} > > R_{am} \quad (1)$$

(where R_{ru} is the dissolution resistance of rutile titania, R_{an} is the dissolution resistance of anatase titania, R_{am} is the dissolution resistance of amorphous titania).

When anodized in H_2SO_4 electrolyte, the increase of the porosity and the pore size with increasing voltage from 90 to 155 V was resulted from more intensive field assisted and chemical dissolution. In addition, because the crystallographic transformation mentioned before has increased the dissolution resistance of the titania layers, the porous structure was not changed obviously with increasing voltage from 155 to 180 V. The anodic layers prepared in H_3PO_4 and CH_3COOH electrolyte in all conditions were all amorphous-like, constant in dissolution resistance. Therefore, the pore size increased continually when applied voltage increased. In CH_3COOH electrolyte, because the dissolve capacity of CH_3COOH (as a mild acid) to titanium oxides layer is relatively weak, the etching of the layer will expand along existed defects. It could result in uneven and larger pores structure, so larger craters and grooves can been obtained (Fig. 5). However, further investigation is required to confirm this hypothesis. According to previous research, the pore size should be larger than 50 μm for soft tissue ingrowths [31]. The results indicate that CH_3COOH, in which anodized titanium oxides layer possessed largest pore size in the given three acid electrolytes, might be a promising electrolyte system to obtain suitable surface-porous implants via anodic oxidation for soft tissue ingrowths. However, more work needs to be done in this field.

3.2 Cell attachment

In order to evaluate the morphology and attachment behavior on the AO titanium substrates, fibroblast cells

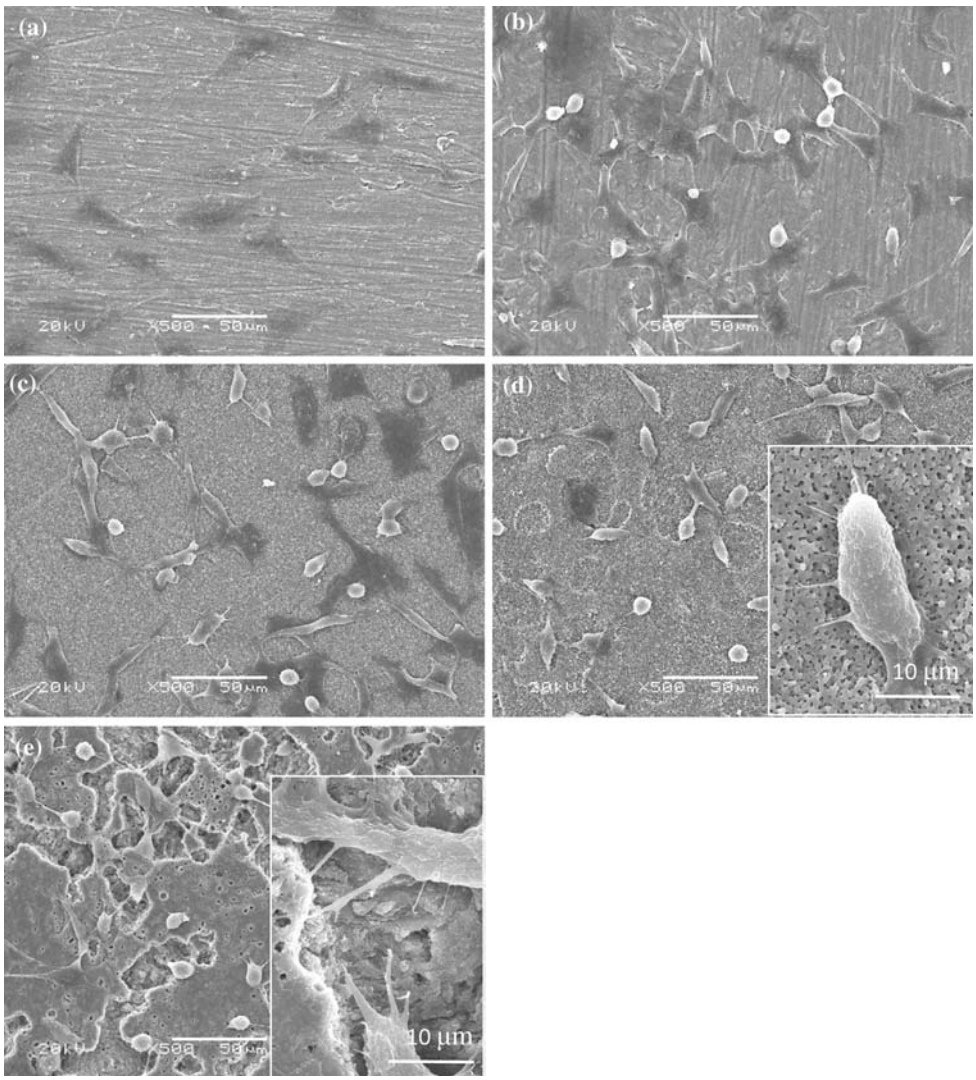

Fig. 6 SEM micrographs of fibroblast cells cultured after 24 h on titanium substrates, **a** untreatment, and anodized at **b** 90 V, **c** 155 V, **d** 180 V in 1 M H_2SO_4, **e** anodized in 2 M CH_3COOH at 180 V and then heat treated at 600°C for 1 h. Insets are high-magnification micrographs

were fixed after 24 h of culture for imaging. At 24 h post-seeding, the cells were rounded and floating in the medium. They gradually adhered and spread out on the substrates surfaces (Fig. 6). Moreover, the cells concentration on the untreated titanium surface is obviously lower than that on the anodized titanium surfaces and the cells concentration on the anodized titanium surface in CH_3COOH is significantly higher than others. From the inset in Fig. 6d, it could be observed that a single cell, which has a spindle shape with long cytoplasmic body, interlocked to micron/nanostructure porous titania surface with filopodia. Figure 6e showed the fibroblasts were anchored onto the facets of the surface of anodized Ti in CH_3COOH, appearing to accommodate the irregularly three-dimensional surface topography, in some cases spanning the pore space. The pseudopod of fibroblast cell also interlocked in the submicron porous edge of craters or grooves, showed in the inset of Fig. 6e.

According to previous reports [35, 36], the growth behavior of fibroblast cells, the osteoblast cells and some other cells in vitro has been shown to depend primarily on the adsorbed vitronectin or fibronectin for the initial adhesion and spreading on materials. Thus, the ability of materials to adsorb such proteins with an active state from serum determines their capacity to support cell adhesion and proliferation, and constitutes an important aspect of their biocompatibility. These proteins are known to become adsorbed on the native titanium surface [36] and the titanium implant with the thicker titania layer is found to have higher biocompatibility [37]. The anodized substrates, which have thicker titania layer, rougher surface morphology and numerous micron pores, compared with untreated substrate, can improve their adsorbing ability for proteins. Moreover, the micron/nanostructure porous edge of the pores is beneficial for cell adhesion [35]. Therefore, during the initial stage, adhesion of cells on untreated titanium surface is less favorable than those on the anodized titanium surfaces, and titanium substrate surface anodized in CH_3COOH is most favorable for cells adhesion. However, this is just a pilot study and further investigation about cells properties on anodized titanium substrates is necessary.

4 Conclusion

Surface-porous titanium samples were prepared by anodic oxidation in H_2SO_4, H_3PO_4 and CH_3COOH electrolytes under various electrochemical conditions. In H_2SO_4 and H_3PO_4 solution, well separated and evenly distributed porous-structure titanium oxides layers can be prepared, with pore size not more than 1 μm. However, a heterogenous porous-structure amorphous titanium oxides layer can be prepared in CH_3COOH electrolytes, with grooves of about 200 μm in length and craters of about 10 μm in diameter. The fibroblast cells experiment show that anodic oxidation of titanium surface can promote fibroblasts adhesion. Anodic oxidation in CH_3COOH electrolyte may be promising to prepare suitable surface-porous implants allowing soft tissue ingrowths. However, further investigation on how to prepare larger and more homogeneous surface-porous Ti implants in CH_3COOH electrolyte via anodic oxidation is necessary.

Acknowledgment This work has been supported by the National Natural Science Foundation of China (project no. 60871062 and 50873066). The supports of Sichuan Province through a Science Fund for Distinguished Young Scholars of Sichuan Province (08ZQ026-007) and Key Technologies Research and Development Program of Sichuan Province (2008SZ0021 and 2006Z08-001-1) are also acknowledged with gratitude. This work was also supported by the Specialized Research Fund for the Doctoral Program of Higher Education from Ministry of Education of China (No. 20070610131). We thank Analytical & Testing Center, Sichuan University for the assistance with the microscopy work. The authors would also like to thank Mrs. Hui Wang of Analytical & Testing Center, Sichuan University for her support and encouragement.

References

1. Van Noort R. Titanium: the implant material of today. J Mater Sci. 1987;22:3801–11.
2. Wang K. The use of titanium for medical applications in the USA. Mater Sci Eng. 1996;213 A:134–7.
3. Brash JL. Biomaterials in Canada: the first four decades. Biomaterials. 2005;26:7209–20.
4. Puleo DA, Kissling RA, Sheu MS. A technique to immobilize bioactive proteins, including bone morphogenetic protein-4 (BMP-4), on titanium alloy. Biomaterials. 2002;23:2079–87.
5. Caulier H, Vercaigne S, Naert I, Waerden JVD, Wolke J, Kalke W, et al. The effect of Ca-P plasma-sprayed coatings on the initial bone healing of oral implants: an experimental study in the goat. J Biomed Mater Res. 1997;34:121–8.
6. Kim HM, Miyaji F, Kokubo T, Nishuguchi S, Nakamura T. Grade surface structure of bioactive titanium prepared by chemical treatment. J Biomed Mater Res. 1999;45:100–7.
7. Kim HM, Miyaji F, Kokubo T, Nakamura T. Effect of heat treatment on apatite-forming ability of Ti metal induced by alkali treatment. J Mater Sci: Mater Med. 1997;8:341–7.
8. Kim HM, Kokubo T, Miyaji F, Nakamura T. Preparation of bioactive Ti and its alloys via simple chemical surface treatment. J Biomed Mater Res. 1996;32:409–17.
9. Liang B, Fujibayashi S, Neo M, Tamura J, Kim HM, Uchida M, et al. Histological and mechanical investigation of the bone-bonding ability of anodically oxidized titanium in rabbits. Biomaterials. 2003;24:4959–66.
10. Yang BC, Uchida M, Kim HM, Zhang XD, Kokubo T. Preparation of bioactive titanium metal via anodic oxidation treatment. Biomaterials. 2004;25:1003–10.
11. Cui X, Kim HM, Kawashit M, Wang L, Xiong T, Kokubo T, et al. Preparation of bioactive titania films on titanium metal via anodic oxidation. Dent Mater. 2009;25:80–6.
12. Oh HJ, Lee JH, Kim YJ, Suh SJ, Lee JH, Chi CS. Surface characteristics of porous anodic TiO_2 layer for biomedical applications. Mater Chem Phys. 2008;109:10–4.

13. Pilliar RM. Powder metal-made orthopedic implants with porous surface for fixation by tissue ingrowth. Clin Orthop. 1983;176:42–51.
14. Gottsauner-Wolf F, Egger EL, Schultz FM, Sim FH, Chao EY. Tendons attached to prostheses by tendon-bone block fixation: an experimental study in dogs. J Orthop Res. 1994;12:814–21.
15. LaBerge M, Bobyn JD, Rivard CH, Drouin G, Duval P. Study of soft tissue ingrowth into canine porous coated femoral implants designed for osteosarcomas management. J Biomed Mater Res. 1990;24:959–71.
16. Bobyn JD, Hacking SA, Tanzer M, Krygier JJ. Tissue response to porous coated acetabular cups: a canine model. J Arthrop. 1999;14:347–54.
17. Kon M, Hirakata LM, Asaoka K. Porous Ti-6Al-4 V alloy fabricated by spark plasma sintering for biomimetic surface modification. J Biomed Mater Res. 2004;68B:88–93.
18. Thelen S, Barthelat F, Brinson LC. Mechanics considerations for microporous titanium as an orthopedic implant material. J Biomed Mater Res. 2004;69A:601–10.
19. Assad M, Jarzem P, Leroux MA, Coillard C, Chernyshov AV, Charette S, et al. Porous titanium–nickel for intervertebral fusion in a sheep model: part 1. Histomorphometric and radiological analysis. J Biomed Mater Res. 2003;64B:107–20.
20. Assad M, Chernyshov AV, Jarzem P, Leroux MA, Coillard C, Charette S, et al. Porous titanium–nickel for intervertebral fusion in a sheep model: part 2. Surface analysis and nickel release assessment. J Biomed Mater Res. 2003;64B:121–9.
21. Wen CE, Yamada Y, Shimojima K, Chino Y, Asahina T, Mabuchi M. Processing and mechanical properties of autogenous titanium implant materials. J Mater Sci: Mater Med. 2002;13:397–401.
22. Zardiackas LD, Parsell DE, Dillon LD, Mitchell DW, Nunnery LA, Poggie R. Structure, metallurgy, and mechanical properties of a porous tantalum foam. J Biomed Mater Res. 2001;58:180–7.
23. Garrett R, Abhay P, Dimitrios PA. Fabrication methods of porous metals for use in orthopaedic applications. Biomaterials. 2006;27:2651–70.
24. Fujibayashi S, Neo M, Kim HM, Kokubo T, Nakamura T. Osteoinduction of porous bioactive titanium metal. Biomaterials. 2004;25:443–50.
25. Park IS, Lee MH, Bae TS, Seol KW. Effects of anodic oxidation parameters on a modified titanium surface. J Biomed Mater Res Part B: Appl Biomater. 2008;84B:422–9.
26. Sul YT, Johansson CB, Jeong YS, Albrektsson T. The electrochemical oxide growth behaviour on titanium in acid and alkaline electrolytes. Med Eng Phys. 2001;23:329–46.
27. Kuromoto NK, Simão RA, Soares GA. Titanium oxide films produced on commercially pure titanium by anodic oxidation with different voltages. Mater Charact. 2007;58:114–21.
28. Zwilling V, Aucouturier M, Ceretti ED. Anodic oxidation of titanium and TA6 V alloy in chromic media. An electrochemical approach. Electrochim Acta. 1999;45:921–9.
29. Sul YT, Johansson CB, Petronis S, Krozer A, Jeong YS, Wennerberg A, et al. Characteristics of the surface oxides on turned and electrochemically oxidized pure titanium implants up to dielectric breakdown: the oxide thickness, micropore configurations, surface roughness, crystal structure and chemical composition. Biomaterials. 2002;23:491–501.
30. Lin CS, Chen MT, Liu JH. Structural evolution and adhesion of titanium oxide film containing phosphorus and calcium on titanium by anodic oxidation. J Biomed Mater Res. 2008;85A:378–87.
31. Oliveira MV, Pereira LC, Cairo CAA. Porous structure characterization in titanium coating for surgical implants. Mater Res. 2002;5:269–73.
32. Sul YT, Johansson CB, Jeong YS, Albrektsson T. The electrochemical oxide growth behaviour on titanium in acid and alkaline electrolytes. Med Eng Phys. 2001;23:329–46.
33. Wu HH, Lu XY, Long BH, Wang XQ, Wang JB, Jin ZS. The effects of cathodic and anodic voltages on the characteristics of porous nanocrystalline titania coatings fabricated by microarc oxidation. Mater Lett. 2005;59:370–5.
34. Dervos CT, Thirios Ef, Novacovich J, Vassiliou P, Skafidas P. Permittivity properties of thermally treated TiO_2. Mater Lett. 2004;58:1502–7.
35. Christenson EM, Anseth KS. Nanobiomaterial applications in orthopedics. J Orthop Res. 2007;25:11–22.
36. Zhang F, Shi ZL, Chua PH, Kang ET, Neoh KG. Functionalization of titanium surfaces via controlled living radical polymerization: from antibacterial surface to surface for osteoblast adhesion. Ind Eng Chem Res. 2007;46:9077–86.
37. Ou KL, Shih YH, Huang CF, Chen CC, Liu CM. Preparation of bioactive amorphous-like titanium oxide layer on titanium by plasma oxidation treatment. Appl Surf Sci. 2008;255:2046–51.